

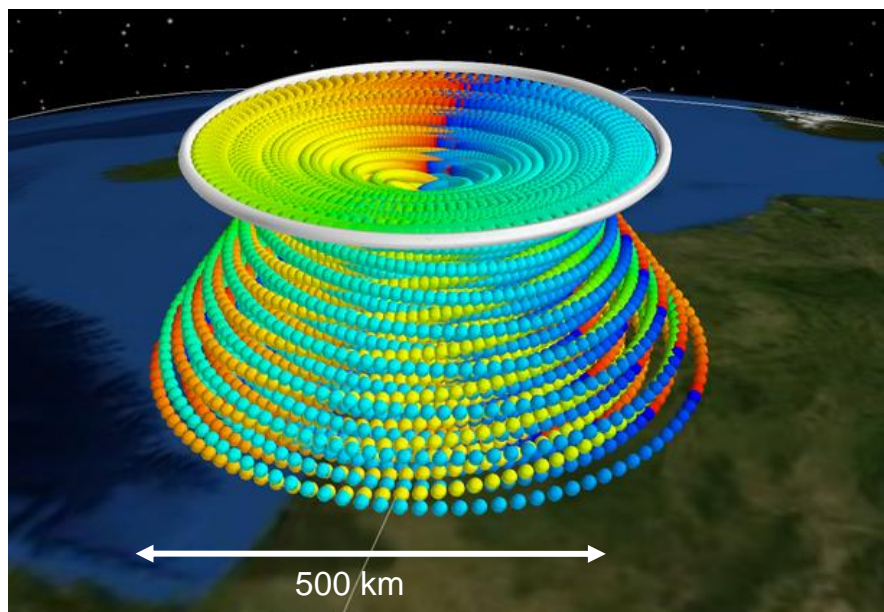
WISE (Wave-driven ISentropic Exchange)

Co PIs: Martin Riese, Martin Kaufmann (FZJ)

and Peter Hoor, Daniel Kunkel (University Mainz)

Instrument Partners: Hermann Oelhaf and Andreas Zahn (KIT), Helmut Ziereis, Andreas Fix and Christiane Voigt (DLR), Martina Krämer and Peter Preusse (FZJ), Volker Ebert (PTB Braunschweig), Andreas Engel (U Frankfurt), Klaus Pfeilsticker (U Heidelberg), Michael Volk (U Wuppertal)

Other contributors to White Book: Peter Spichtinger (U Mainz), Felix Plöger, Reinhold Spang, Paul Konopka, Bärbel Vogel, and Rolf Müller (FZJ)



“White Book”

Januar 24, 2017

1 State-of-the-art and preliminary work

1.1 Introduction

Changes of the distributions of trace gases, like water vapor, ozone and ozone depleting substances, and thin cirrus clouds in the upper troposphere and lower stratosphere (UTLS) strongly impact radiative forcing of the Earth's climate and surface temperatures (Riese et al., 2012, Hossaini et al., 2015), and are of key importance for understanding climate change (Hegglin and Shepherd, 2009; Solomon et al., 2010). Transport and mixing in the extratropical upper troposphere / lower stratosphere (ExUTLS) play a key role for the quantitative understanding of the distribution of these radiatively active species (Gettelman et al., 2011). The formation of the extratropical transition layer (ExTL) around the tropopause, which exhibits chemical characteristics of both the stratosphere and the troposphere (Hoor et al., 2002, 2004; Pan et al., 2004), is a direct consequence of the underlying frequent small scale mixing processes. Coupled climate chemistry models (CCMs) are capable of simulating the overall structure of the ExUTLS region, but exhibit deficiencies when looking at the underlying processes (Strahan et al., 2007, Hegglin et al., 2010). These are partly related to the sub-grid nature of these processes which in turn introduce errors to the distribution of tracers.

The processes influencing the extra-tropical UTLS are summarized in *Gettelman et al., (2011)* and illustrated in *Fig.1 and Fig.2*. In this proposal, we address 4 different scientific themes (STs), which are introduced in Section 2 in conjunction with our preliminary work.

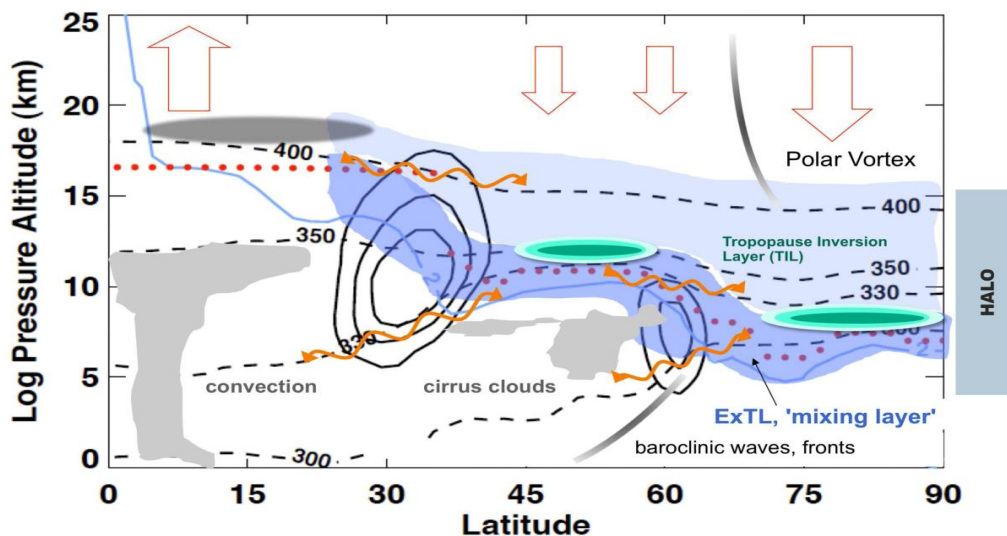


Figure 1: Schematic of the Extra-tropical UTLS. Major ExUTLS features like the extra-tropical transition layer (ExTL) and the Tropopause Inversion Layer (TIL) are described in the text. The lowermost stratosphere (LMS) is the region in the extra-tropical stratosphere that is directly connected with the troposphere by isentropic surfaces. Wind contours (solid black lines 10ms^{-1} interval), potential temperature surfaces (dashed black lines), thermal tropopause (red dots) and potential vorticity surface (2PVU: light blue solid line) represent data from a cross section along 60° longitude on February 15, 2006. (Figure from Gettelman et al., 2011).

Particularly at the tropopause these uncertainties of the mixing processes lead to large uncertainties of radiative forcing estimates and thus the prediction of future developments of the composition and temperature structure of the ExUTLS (Riese et al., 2012). It is therefore of great importance to

quantify the physical and chemical processes (e.g. exchange of air masses, cirrus formation) as well as the source regions and transport times that govern the composition of the UTLS.

In the ExUTLS, which is the focus of the WISE proposal, air is a mixture of aged air masses, which have been transported with the stratospheric (Brewer-Dobson) circulation through the deep stratosphere, and of young air masses crossing the tropopause. Potential source regions are the tropical tropopause and the subtropical jet with strong seasonal dependencies (Hoor et al., 2005, Bönisch et al., 2009). During summer the Asian summer monsoon constitutes an additional pathway for transport into the extratropical UTLS, which also transports large amounts of pollutants and water vapor up to altitudes of 18 km (or potential temperature ranges up to 390 K), which can efficiently contribute to the lower stratospheric trace gas composition (e.g. Konopka et al., 2009, 2010; Randel, et al., 2010). Thus, this season is of particular importance for the distribution of water vapor and its effect on the lower stratosphere (Ploeger et al., 2013). In fact the latitudinal and seasonal variations of water vapor at 390 K (Randel and Jensen, 2013) show that the air masses with highest moisture content in the stratosphere do not originate in the tropics but rather above the Asian monsoon.

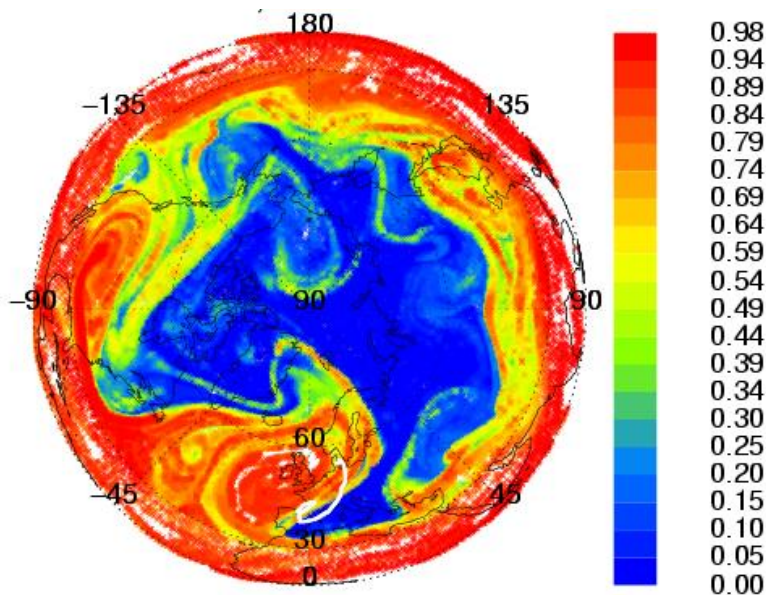


Figure 2: Illustration of wave-driven exchange of air masses across the subtropical jet for the 350K isentropic surface by means of a CLaMS simulation for autumn conditions. Shown is the fraction of tropospheric air. Note the strong disturbances of the subtropical jet (tropopause) by Rossby wave activity, in particular over the Atlantic, and the associated filamentary structures of air with large tropospheric contributions that extend deep into the extra-tropical lowermost stratosphere (blue area).

The local effect of strong water vapor gradients at the tropopause includes a strong modification of the local radiation budget and thus the temperature profile in the tropopause region, thereby altering the static stability (given as the squared Brunt Väisälä frequency N^2) in the lowermost stratosphere. A key feature of the thermodynamical structure of the extratropical tropopause region is the tropopause inversion layer (TIL) (Birner et al., 2002, 2006), which constitutes a region of high static stability just above the thermal tropopause (Grise et al., 2010). It undergoes a seasonal cycle with a maximum in the summer mid- and high latitudes (Grise et al., 2010) as well as showing

latitudinal dependencies (Bell and Geller, 2008). Several authors pointed out that the vertical structure of trace gases like CO or ozone are related to the location of the TIL (Kunz et al., 2009, Hegglin et al., 2009). Hoor et al., (2010) found that the CO gradient in the ExUTLS coincides with a change of transport time from the troposphere. This suggests that trace gas distributions and the physical properties of the TIL are linked to each other. The coupling between constituents and TIL is at least partly established by vertical gradients of radiatively active species like H₂O and ozone which modify the static stability (Randel, 2007). Thus an effect of atmospheric constituents on the TIL is evident, but in turn a direct impact of the TIL on transport and mixing is still an open question.

1.2 Scientific themes

The scientific topics of WISE cover the following four main scientific research themes as described in more detail below:

ST1: Transport and mixing in the region of the ExTL and the influence of the tropopause inversion layer (TIL)

Notably, the ExTL and the TIL appear to be interconnected. Miyazaki et al., (2010) concluded from high resolution model simulations that the seasonality and thermodynamic structure of the TIL and the chemical structure and mixing processes leading to the ExTL are similar because of common underlying dynamic processes. On the basis of ACE-FTS satellite data sampled over several years, Hegglin et al., (2009) found a collocation of the maximum vertical gradient of mean CO profiles in the extra-tropics and the location of the TIL. However, the results from satellite platforms are limited by resolution and sampling frequency and do not allow to infer detailed process understanding on the local scale, which requires a systematic investigation using high resolution in-situ or high-resolution remote sensing data.

Kunz et al., 2009 used SPURT in-situ data to analyze the relation between static stability, characterizing the TIL, and the CO-O₃ correlation, characterizing the ExTL, and found indications for different strengths of mixing relative to the location of the TIL. They also highlighted the role of baroclinic wave breaking for their case study, which is in agreement with the results of Wirth and Szabo (2006) and Erler and Wirth (2010). A detailed view on the role of water vapor during baroclinic life cycles reveals a very complex interplay between water vapor on the formation and maintenance of the TIL, which depends on the stage of development and phase of the life cycle (Kunkel et al., 2016).

Particularly, synoptic processes which modify potential vorticity (PV) in the mid latitude troposphere may contribute to a diabatic change of PV and potentially static stability at the tropopause (Joos and Wernli, 2012, Chagnon et al., 2013). A diabatic change of PV is associated with tracer exchange across the dynamical tropopause. However, detailed measurement studies are missing, which address the contribution of these synoptic scale processes to the variability of static stability and tracer exchange across the tropopause.

Above the ExTL, the isentropic PV gradient at the subtropical jet determines the gross composition of the extratropical UTLS, which also provides a strong link to the Asian summer monsoon. In particular,

the Asian monsoon lifts moist air into the sub-tropical upper troposphere, where it modifies the radiation budget and heating rates, which in turn modify static stability on the large scale.

Several mechanisms which may contribute to the formation of the TIL have been discussed: enhanced static stability in the extratropics might be partly the result of the residual circulation (Birner, 2010) or baroclinic wave breaking events in the extratropics (Wirth, 2003; Son and Polvani, 2007; Erler and Wirth, 2010). The synoptic scale behavior of the TIL can be modified by breaking gravity waves locally enhancing the strengths of the TIL persistently (Kunkel et al., 2014). As first proposed by Randel et al. (2007), relaxation into a radiative equilibrium might serve as main mechanism forming and maintaining the TIL in the extratropics, particularly in the summer hemisphere. The impact of radiatively active species like water vapor and ozone, and species affecting ozone on the temperature structure further makes the TIL a sensitive indicator for changes of ozone chemistry or changes of tropopause temperatures.

ST2: Horizontal Transport into the extratropical lower stratosphere above the ExTL

Above the ExTL breaking Rossby-waves provide a mechanism for stirring of air masses and for quasi-horizontal isentropic exchange between tropics and extra-tropics (e.g., McIntyre and Palmer, 1983; Riese et al., 2002). Related intrusions of low latitude air may reach deep into mid and high latitudes (e.g., Pan et al., 2009). The seasonality of horizontal transport depends on the strength of the subtropical jet, which acts as transport barrier, which is weakest in the summer hemisphere (Haynes and Shuckburgh, 2000).

In a recent paper, Homeyer and Bowman (2012) showed that the seasonality of poleward transport related to Rossby-wave breaking reverses at altitudes above 420 K: above 420 K, horizontal transport maximizes during hemispheric winter (Vaughan, 1996; Postel and Hitchman, 1999), and below transport maximizes during hemispheric summer and fall. Rossby-wave breaking in the northern hemisphere lower stratosphere during summer/fall coincides with the highest water vapor mixing ratios in this season. Consequently, horizontal poleward transport by Rossby-wave breaking (RWB) acts to moisten the mid latitude UTLS in boreal summer (e.g., Rosenlof et al., 1997; Pan et al., 1997). Predominant regions of RWB are the Northern Atlantic and Pacific (e.g., Postel and Hitchman, 1999; Homeyer and Bowman, 2012). A related mechanism for moistening the lowermost part of the extratropical UTLS during summer has been proposed by Dethof et al. (1999), involving mid latitude synoptic disturbances interacting with the Asian monsoon anticyclone. During these interactions moist air filaments are drawn out of the anticyclone and transported into NH extra-tropics.

Recent observations from MLS (Microwave Limb Sounder) and simulations with CLaMS (Chemical Lagrangian Model of the Stratosphere; Konopka et al., 2010) indicate that upward transport of water vapor within the Asian and American monsoons and subsequent horizontal poleward transport serve as the dominant pathway of water vapor into the mid latitude UTLS during boreal summer and fall (Konopka et al., 2010, Ploeger et al., 2013, Randel and Jensen, 2013, see also Fig.3). Day-to-day variability in observed and simulated zonal mean water vapor and ozone time series corroborates the finding that horizontal transport to high latitudes occurs abruptly within deep intrusions of low latitude air, which are likely related to Rossby-wave breaking (see Fig.4, Vogel et al., 2016). The filamentary nature of water vapor transport to mid latitudes is reflected in the large variability of water vapor mixing ratios observed in the mid latitude UTLS as well as anti-correlated mixing ratios

(Ungermaann et al., 2013). Furthermore, tagged tracer studies with the CLaMS model highlight the role of the Asian monsoon for the composition of the LMS (Ploeger et al., 2013; Vogel et al., 2014).

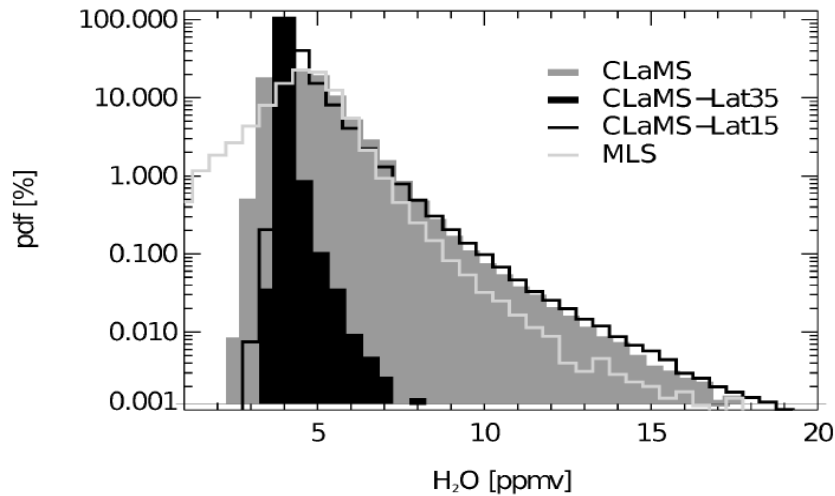


Figure 3: Probability density function (pdf) of water vapor mixing ratios in NH mid latitudes (40 to 70° N latitude, 370 to 420 K) for July to October (2005/2006) climatology. CLaMS reference simulation as gray shading, the sensitivity simulations with barriers at 35 degree N (15 degree N) as black shading (black line), MLS observations as light-gray line. Obviously, all high mixing ratios vanish with a transport barrier along 35°N, and hence turn out to be linked to horizontal transport from low latitudes. Figure adapted from Ploeger et al. (2013).

Comparisons of N₂O and CO during TACTS/ESMVal with CLaMS backward trajectories show that the Asian monsoon substantially contributes to the observed tracer signatures during summer (Müller et al., 2016, Vogel et al., 2014; 2016). Some halogenated gases of anthropogenic origin, e.g. C₂Cl₄ may also serve as tracer of recent transport from anthropogenically influenced regions like the Asian monsoon area.

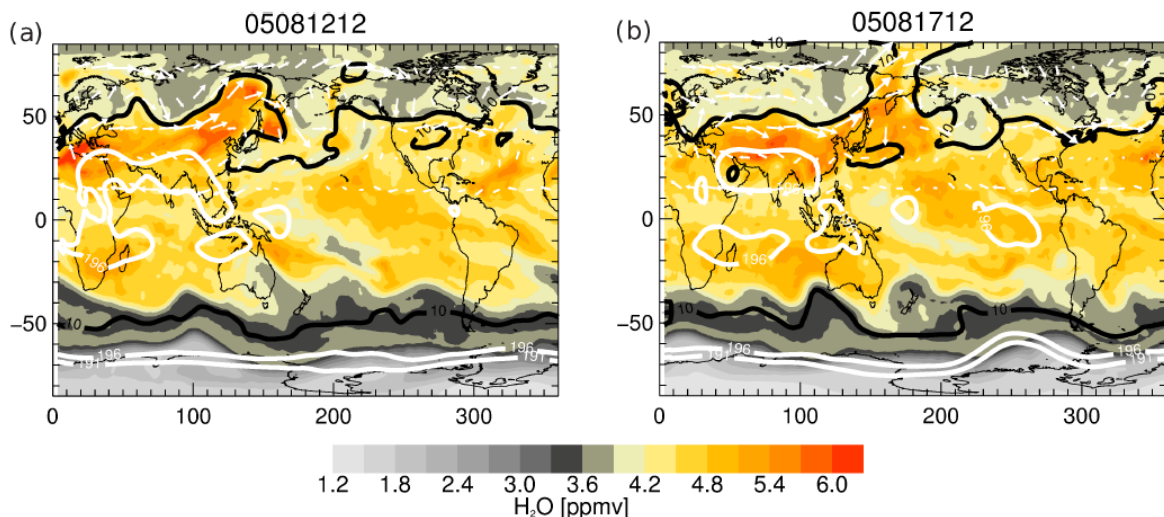


Figure 4: Water vapor distribution at 400K for 12 (a) and 17 (b) August 2005, from the CLaMS simulation. The black line is the 10 PVU, the white line the 196K temperature contour and the white arrows the horizontal wind on the NH (v scaled by factor 3). The figure sequence shows a poleward intrusion of moist air from low latitudes around 150 degree E. Figure adapted from Ploeger et al. (2013).

The measurements to be performed within WISE will not only allow for differentiating between various transport pathways but also for quantifying transport time scales. The mean age of air can be determined from very long lived tracers like e.g. SF₆ and CO₂. Species with chemical loss, e.g. short lived halocarbons, can also be used to derive information on transport time scales. Observations of a range of species with different chemical lifetimes can thus be used to derive information on the transit time distribution of troposphere-stratosphere transport (TST), the so-called age spectrum (e.g. Ehhalt et al., 2007).

ST3: The role of halogenated VSLs for ozone and radiative forcing in the UTLS region

Recent observations show that halogenated very short lived substances (VSLs) are also an important source of stratospheric halogens, and in particular for the halogen budget of the UTLS and thus for the budget of ozone there (WMO-2014, Hossaini et al., 2015; Werner et al., 2015). Major pathways for transporting ozone destroying substances and in particular of the brominated VSLs into the UTLS and ExTL are thought to be the Western Pacific during the convective season, the Asian Monsoon, as well as the quasi isentropic transport across the subtropical jet (e.g. Levine et al., 2007; Aschmann et al., 2009; Pisso et al., 2010; Liang et al., 2014). The potential of the halogenated VSLs for considerably affecting ExTL ozone and thus radiative forcing by ozone comes through their short atmospheric lifetime. In fact recent chemical transport model (CTM) simulations indicate that ozone loss from VSLs had a radiative effect nearly half of that from long-lived halocarbons in 2011 and has contributed a total of about -0.02 W/m^2 to global radiative forcing (Hossaini et al., 2015) since pre-industrial times. These calculations however did not consider the effect on ozone of inorganic bromine directly transported into the lowermost stratosphere. Evidence for the latter contribution to stratospheric bromine mostly came through simultaneous balloon-borne and air-borne measurements of total organic and inorganic species in the stratosphere (e.g. Pfeilsticker et al., 2000; Dorf et al., 2008; Laube et al., 2008; Brinckmann et al., 2012; Sala et al., 2014, WMO-2014), and by our recent measurements of the inorganic bromine budget at stratospheric entry level over the Eastern Pacific (Werner et al., 2015). While the former studies indicated a range of 0 – 5 ppt for the inorganic bromine mostly entrained from the tropical troposphere into the stratosphere (WMO-2014), the latter most recent study could establish a smaller range (2.63 +/-1.04 ppt) (Werner et al., 2015). In as much the transport processes of the ExTL contribute to inorganic bromine either directly injected by inorganic bromine species from troposphere, or by VSLs, and thus to ozone loss in the UTLS is however to date unclear.

ST4: Occurrence and effects of sub-visual cirrus (SVC) in the lowermost stratosphere

The imprint of various water vapor pathways into the lowermost stratosphere (LMS) on sub-visible cirrus formation has been investigated in a number of studies (e.g. Dessler, 2009, Montaux et al. 2010, Pan and Munchak, 2011, Wang and Dessler, 2012). The formation of cirrus clouds above the mid-latitude tropopause is discussed therein quite controversially. In-situ observations of cirrus clouds in the stratosphere are sparse (Müller et al., 2015a). Dessler (2009) found relatively high occurrence rates of cirrus above the mid and high latitude tropopause based on space borne lidar data of the CALIOP instrument on the CALIPSO satellite, even 0.1% at 3 km or 40-50 K potential temperature above the tropopause. Pan and Munchak (2011) showed that accurate tropopause definition and coordinates relative to the tropopause are important for this type of analysis and lead to significant differences in their conclusions. The authors found a substantial fraction of cases in the

tropics showing occurrence of cirrus in the stratosphere for example in the western Pacific between the cold point tropopause (CPT) and the lapse rate tropopause (LRT) (up to 2.5 km above the LRT). The authors speculated that most of these clouds were triggered by gravity wave induced temperature disturbances, which typically are observed above areas of deep convection.

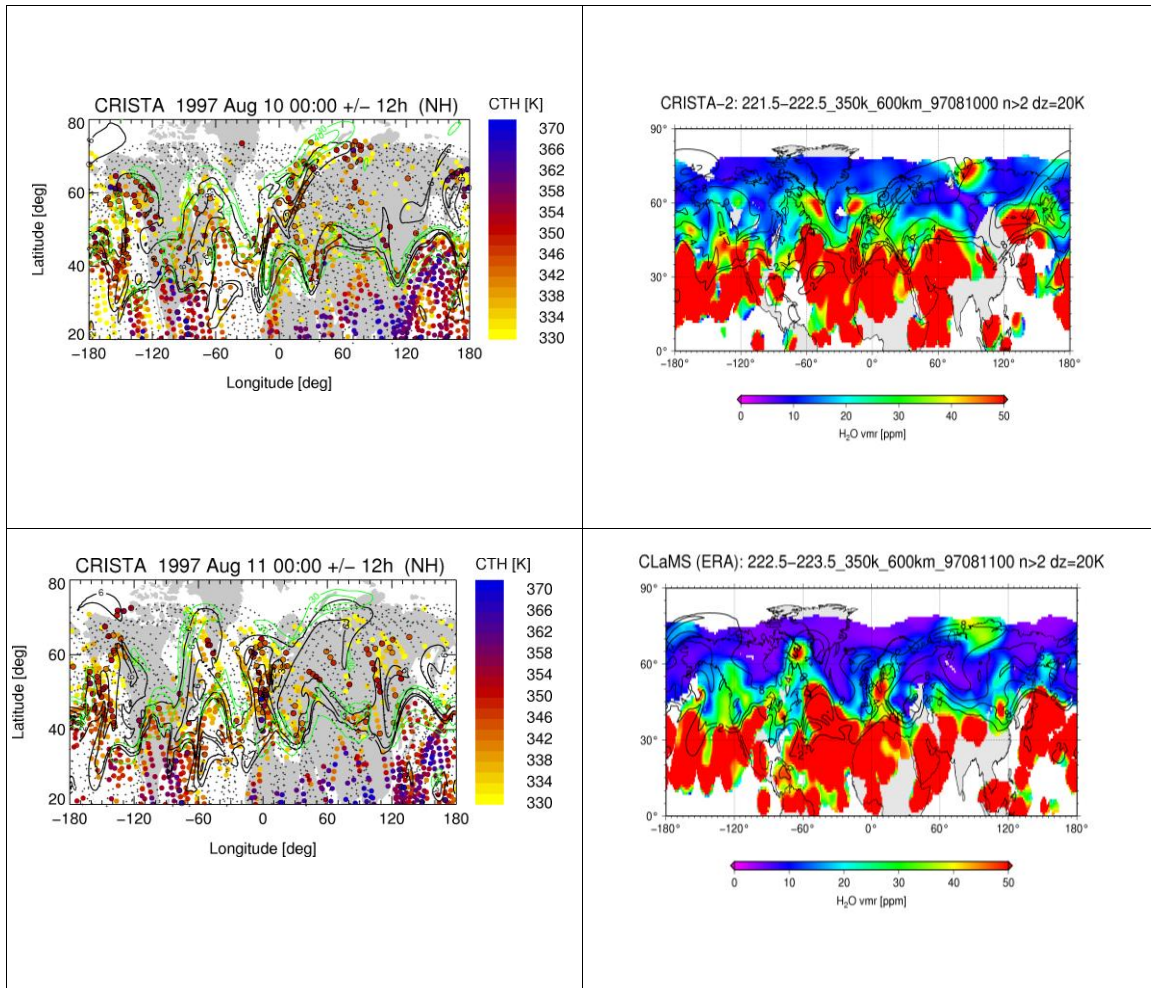


Figure 5: Cloud top height observations in Θ -coordinates during the CRISTA-2 mission (left) and corresponding gridded water vapor measurements at 350K for Aug 10 and 11 1997. Super-imposed ERA interim PV (black) and horizontal wind contours (green).

Ground based cloud observations from mid latitude lidar stations show frequent cirrus events at and above the tropopause (Keckhut et al., 2005). Many of them coincide with the observations of a secondary tropopause (Noël and Haefelin, 2007). Isentropic transport and mixing of subtropical air masses of tropospheric high water values into the UTLS may give rise to these cirrus. Eixmann et al. (2010) investigated the dynamical link between the poleward Rossby wave breaking (RWB) events and the occurrence of upper tropospheric cirrus clouds for lidar measurements above Kühlungsborn (54.1°N, 11.8°E). For three similar cirrus events they found a strong link between low values of potential vorticity (proxy for RWB activity), enhanced up-draft velocities, and cloud ice water content.

Rolf et al. (2012) used ground based LIDAR and identified cirrus occurrence +/- 500m around the tropopause over Jülich, Germany (50.9°N, 6.4°E) and in 5% of the cases above the tropopause. IR

limb observations of cirrus clouds during the CRISTA-2 mission in 1997 suggest also frequent cirrus events around the mid latitude tropopause (Spang et al., 2002). Recent investigations with the CRISTA-2 dataset show a significant amount of these cirrus well above the mid and high latitude tropopause. Corresponding water vapor observations and meteorological analysis suggest a link between isentropic transport of subtropical air masses at 350 K and cirrus formation at mid and high latitudes associated with the poleward transport of subtropical air masses (Spang et al., 2015). A preferential region for LMS cirrus above the north Atlantic to Scandinavia region is identified in preliminary analyses of CRISTA-2 and MIPAS Envisat cloud observations (Spang et al., 2015), an area well known for high activity in RWB in the UTLS (e.g. Homeyer and Bowman, 2012) and also for warm conveyor belt (WCB) occurrence in the troposphere (Eckhardt et al., 2004). WCB events seem to trigger cirrus cloud formation in the upper troposphere (Spichtinger et al., 2005).

Although there are a couple of ground based observations and indications in the satellite data suggesting the presence of cirrus clouds in the LMS, there is almost no unambiguous prove of their existence and many open questions with respect to how these clouds may form in the LMS are open. An important question is, for example, which specific meteorological conditions facilitate the formation of ice particles in this specific region, how frequently do these cirrus clouds occur, and do part of these clouds occur significantly above the tropopause. Intensive airborne measurements with the long range HALO aircraft with an optimised remote sensing payload in regions with high mid latitude UTLS cirrus occurrence will improve the knowledge about these so far disputable cirrus cloud observations.

2 Scientific objectives and questions

As outlined above the WISE consortium has identified four major research topics, which will be addressed within the project. Specifically, the consortium identified the following main science questions for each of the scientific topics to be addressed in WISE as given below:

ST1_Q1: Does the TIL affect transport and mixing into the lower stratosphere and within the lower stratosphere?

The TIL is at least partly affected by radiation effects from the strong gradients of water vapor and ozone. To what extent the TIL in turn affects the distribution of trace gases or acts on vertical transport is entirely open. The coincidence of the TIL location and the region of strongest trace gas gradients might indicate such a relation.

ST1_Q2: Which factors determine the formation of the TIL and how do these in turn affect transport?

Three major factors are discussed to affect the occurrence of a TIL and modify the static stability of the tropopause region: large scale dynamics, radiative effects and dynamical processes associated with baroclinic wave breaking events. The relative importance of each process is yet unknown.

ST2_Q1: What is the impact of wave-driven large scale eddy mixing on the composition of the mid-to high-latitude LMS?

For NH mid and high latitudes, simulations show a clear anti-correlation between water vapor and ozone daily tendencies up to altitudes of 450K during summer. This reveals a large influence of

frequent horizontal transport events from low latitudes that will be confirmed by high-resolution aircraft observations. One focus will be on the quantification of the relevant time-scales of transport. The effect of downward transport by the Brewer-Dobson circulation (BDC) can be separated based on typical stratospheric or age tracers.

ST2_Q2: What is the role of the Asian Monsoon in moistening the extratropical UTLS in summer?

Zonally averaged satellite observations suggest a dominant transport pathway for moistening the extratropical UTLS during summer and fall related to the Asian monsoon and horizontal poleward transport. However, the underlying transport structures (including time scales of transport) cannot be resolved by current satellite observations and must be quantified based on high-resolution aircraft measurements.

ST2_Q3: What are typical time scales for mixing and how are these related to the underlying dynamical processes and source regions?

Large scale processes associated with wave breaking as well as small scale processes at the local tropopause interact and finally lead to an exchange of trace gases on different temporal and spatial scales. The details of this interaction of scales as well as their relation to possible source regions and processes is yet unclear and will be investigated by combinations of high resolution tracer measurements of different lifetimes.

ST3_Q1: To what extent contribute transport processes in the ExUTLS to the halogen budget of the LMS and what is their effect on ozone?

Observations and modeling of the stratospheric halogen budget suggest a considerable role of VSLS and their inorganic product gases for the budget of bromine and possibly iodine. In addition recent model calculations indicated that these species play a significant role for LMS ozone and thus radiative forcing. To date it is unclear how much these ozone depleting species are transported across the extratropical tropopause and affect ozone in the LMS.

ST4_Q1: What is the link between Rossby wave breaking events and associated transport of water vapor and cirrus formation at mid latitudes?

Cirrus formation at mid latitudes is influenced by the large-scale meteorological situation. Water vapor transport from the subtropics by Rossby wave breaking plays an important role, which is not yet quantified (Link to ST1 and ST2). It is also not yet clear, whether water vapor transport by Rossby wave breaking facilitates the formation of sub-visible cirrus clouds even in the-extratropical lowermost stratosphere.

ST4_Q2: What is the impact of cirrus at, and above the mid-latitude tropopause on the radiation budget and on stratospheric water vapor gradients?

Even though the influence of cirrus near the mid latitude tropopause on the upward water vapor transport through the tropopause is expected to be small, they might contribute to the vertical water vapor gradient. Both cirrus particles as well as the water vapor gradient affect the radiation budget and thus the local temperature structure. Information about cirrus cloud occurrence in the stratosphere is still limited and therefore needs to be quantified to estimate this effect

3 Observational requirements

Platform

The extratropical UTLS region is the key region for the scientific questions of the WISE consortium. HALO with its capabilities and the successfully flown instrumentation during TACTS, on which the proposed payload is largely based, constitutes the ideal platform to address these questions. The aircraft is capable of carrying a payload up to altitudes of 15.5 km or Theta = 420 K which is above the LMS in mid latitudes. It is therefore the ideal tool to investigate the vertical temperature and trace gas structure in the extra-tropical UTLS and the interaction between important processes.

Instrumentation

WISE aims to quantify the relationship between trace gas exchange/mixing (ExTL) and static stability (TIL) (ST1). In addition, the influence of Rossby wave breaking (RWB) events on horizontal transport of water vapor and into the LMS shall be investigated as well as its relationship to the formation of sub-visible cirrus (ST2, ST4). All these objectives require a unique set of 3D measurements of temperature and static stability (N^2), various trace gases (e. g. water vapor, ozone, tracers), and cirrus clouds obtained from remote sensing instruments of unprecedented resolution and data coverage, in combination with high precision in-situ observations. The 3D measurement capabilities of the new GLORIA infrared limb imager (see *Figure 6*) play an important role for the quantification of dynamical structures (e.g. N^2) and trace gas structures associated with cross-tropopause exchange. In-situ observations provide detailed information on mixing processes and tracer structure with high spatial resolution, which is essential to perform tracer-tracer analyses (e.g. CO-O₃ correlations). A unique combination of limb and nadir remote sensing instruments (IR limb imaging/ lidar / uv-vis) will be used for innovative studies of optically and vertically thin cirrus clouds in the UTLS region. A complete list of the instruments is given in Appendix A

Campaign location and season

The evolution of baroclinic life cycles and RWB events and their role for cross tropopause exchange can be best observed over the Atlantic. This includes the interaction of water vapor transport (ST1, ST2) with the TIL (ST1) as well as the transport VSLs's (ST3) and the formation of SVC (ST4). An optimal campaign base would be **Ireland** with the opportunity to cover the evolution of baroclinic waves over the North Atlantic as well as to study exchange close to the subtropical jet (Fig.6) . This would allow to follow the temporal evolution of tracer structure and the TIL on subsequent days during wave breaking events. The best season for the observations is the transition from summer to autumn. The largest water vapor values in the UTLS occur during September/October (ST1, ST2, ST3). This is a result of

wave-driven transport of water vapour, which is large from July until October in this altitude region (ST1, ST2). September/October is also clearly the best period to investigate the impact of the Asian monsoon summer outflow on the composition of the LMS and to quantify the import of VSLs into the extratropical UTLS via the subtropical jet or the monsoon system (ST4).

Flight strategy and number of flight hours

Investigations of the evolution of baroclinic life cycles and RWB events and their role for cross tropopause exchange are in the center of WISE. During baroclinic wave breaking events strong modifications of stability and exchange can be expected in a rather short time period (days). To capture this temporal evolution of the underlying dynamical processes measurements of related tracer structures during subsequent days will be performed. In addition, the tropopause region and the UTLS and TIL will be investigated under cyclonic and anti-cyclonic conditions as well as during relatively calm or less dynamically disturbed (background) synoptic situations. Potential flight tracks are shown in Figure 6. In total, we plan with about 110 flight hours.

The initial flight planning will primarily focus on the most dynamic regions, where also the most pronounced horizontal transport and mixing (e.g. H₂O) can be expected as well as the formation of sub-visible cirrus (SVC). Extended tomographic remote-sensing observations are planned under this condition to study wave breaking and associated transport in 3 dimensions. Corresponding mixing effects will also be analyzed using classical tracer correlations [e.g. CO and ozone] on the basis of in-situ aircraft measurements.

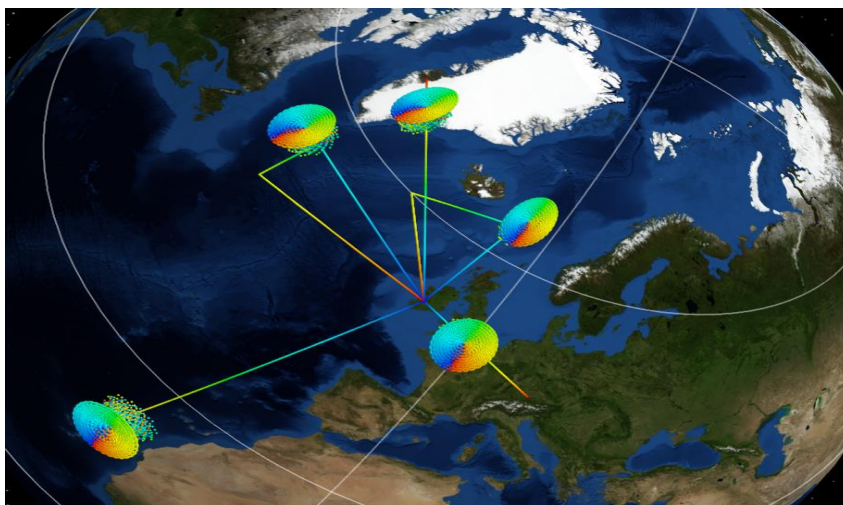


Figure 6: Potential flight tracks during WISE from Ireland as the main campaign base. The colored areas indicate tomographic flight patterns.

A typical flight pattern is shown in *Figure 7*. For an optimal use of the remote sensing instrumentation, HALO will fly at the highest possible flight level (~15 km) most of the time. For each flight, we plan at least one tomographic observation of an active region in combination with a dive in order to optimally exploit the synergies between remote-sensing and in-situ instruments

In order to observe the horizontal and vertical structures (2D curtains) by in-situ instruments, a grid type flight pattern with multiple vertically stacked horizontal legs of e.g. 30 minutes can be implemented. These flight legs will characterize the chemical composition of the region of interest over a given time period. During the first and the last leg (and possibly at intermediate intervals) dropsondes will provide a detailed view of the thermal structure of the tropopause region and the temporal evolution of the structures, occurring during the stacked measurements. The pattern would complement the tomographic capabilities of GLORIA (Fig.8) and also serve for extensive validations.

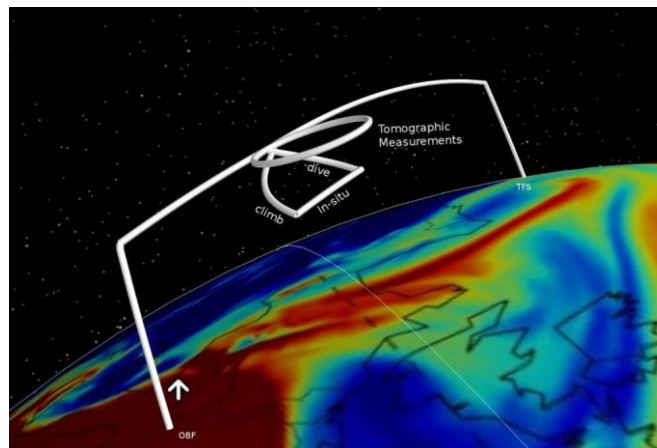


Figure 7: Typical flight pattern for WISE

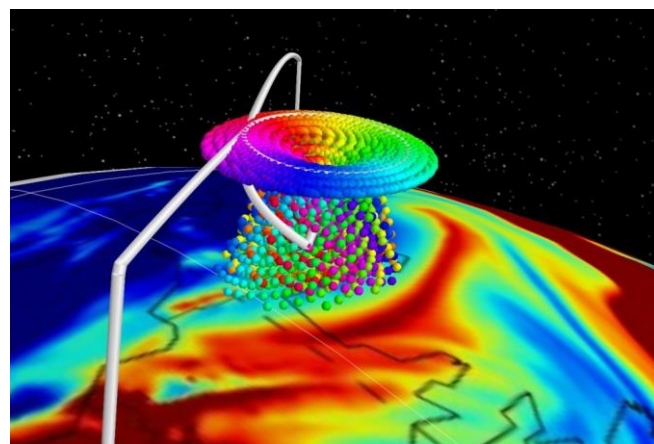


Figure 8: Typical measurement pattern of the IR limb imager (GLORIA). The synergetic use of remote sensing and in-situ measurements is an important feature of the mission. The

structure of the LMS is illustrated by means of ozone fields obtained from GEMS-AQ simulations (Struzewska and Kaminski, 2008).

Instruments and models

To fulfill the science objectives, the following quantities are needed:

- Three-dimensional fields of water vapor, ozone, and transport tracers obtained from remote sensing, complemented by highly precise in-situ observations (H₂O, O₃, CFCs, N₂O, CH₄, CO₂, CO, HCl, short lived tracers)
- Three-dimensional fields of temperature (and static stability), complemented by profile data with high vertical resolution (drop sondes)
- Macro-physical cloud properties (cloud top and base height, horizontal extent)
- Micro-physical cloud properties (slanted and nadir ice water path, ice water content, cloud extinction, cloud effective particle radii)

This will be realized by the following set of instruments:

GLORIA:

- Three-dimensional measurements of H₂O, O₃, CFC11/12 and other tracers with high spatial resolution (ST1, ST2, ST4)
- Three-dimensional distributions of temperature and static stability (ST1)
- Three-dimensional structure of clouds including cloud top and cloud base; limb/slant ice water products, cloud type classification (ice, aerosol, ash); ice water content and mean radii estimates (ST4)

Dropsondes:

- Pressure/temperature/humidity/wind profiles with high vertical resolution (ST1)

WALES

- Two-dimensional curtains of H₂O and O₃ (ST1, ST2, ST3) and SVC properties (ST4)

Mini-DOAS:

- Vertically resolved information on cirrus occurrence and gas phase water vapour (ST1, ST4) and brominated VLS (ST3)

FISH, HAI:

- In-situ measurements of total water, gas phase water, and ice water content (ST1, ST2, ST4)

GhOST-MS:

- SF₆, CFC-12, halogenated VLS, (ST1, ST2, ST3)

HAGAR-4:

- In-situ measurements of CO₂, SF₆, CH₄, N₂O, CFC-11, CFC-12, Halon-1211 and several short-lived NMHCs (ST1, ST2)

AIMS:

- HCl (ST2, ST3) or alternatively water vapor and total water (ST1, ST2, ST4)

UMAQS:

- CO, N₂O, CO₂ (ST1, ST2, ST4)

FAIRO:

- O₃ (ST1, ST2, ST3)

AENEAS

- NO, NO_y (ST1, ST2)

Supplementary data:

- Near real time cloud fields for spotting regions of UTLS cirrus activity (CALIPSO)
- Geostationary data of tropospheric cloud and water vapour channels

Forecasts

Forecasts of meteorological parameters and the relevant chemical composition and post-flight data analyses will be provided during the aircraft campaign period to support the scientific flight planning. Core model of the parameter forecast is the **Chemical Lagrangian Model of the Stratosphere (CLaMS)**, which is the first Chemistry Transport Model (CTM) based on Lagrangian transport where the concept of a deformation-induced mixing was successfully realized both in 2 and 3 dimensions (*McKenna et al. JGR, 2002, Konopka et al. JGR, 2004*). CLaMS is based on a Lagrangian formulation of the tracer transport and, unlike Eulerian CTMs, considers an ensemble of air parcels on a time-dependent irregular grid that is transported by use of the 3-D-trajectories. The irreversible part of transport, i.e. mixing, is controlled by the local horizontal strain and vertical shear rates with mixing parameters deduced from observations. This physically motivated parameterization of mixing can be varied in a broad range, from a no-mixing case to an exaggerated mixing (*Konopka et al., 2004; 2007*). By this approach, the impact of the most uncertain components of transport (i.e. vertical velocities and mixing) on the distribution of all relevant species can also be analyzed. Global and high resolution (up to 20 km/few 100m – horizontal/vertical resolution) simulations with the most recent version of CLaMS (*Konopka et al., ACP, 2007*) covers both the troposphere and the stratosphere and will be utilized in the framework of this project for forecasts as well as for analyses of the results. Model parameters are provided for potential flight times by the reverse domain filling method (RDF) using CLaMS trajectories.

Further, predictions of the formation of cirrus clouds can be provided by the model **CLaMS-Ice**, that uses a two-moment bulk cirrus formation scheme (Spichtinger and Gierens, 2009) along CLaMS trajectories. CLaMS-ice was developed withing the DFG HALO SPP and has been used in the flight planning for the HALO campaigns ML-Cirrus and POLSTRACC.

Model and forecast data can be displayed using a flight planning tool called **Mission Support System (MSS)**, a program that displays horizontal and vertical cuts (along a proposed flight path) of different forecast model parameters that hosted on a web-map server. This program has recently been extended such that for example also CLaMS data and the position of the GLORIA tangent points can be displayed.

4 Planned Scientific analyses

ST1_Q1:

The temporal evolution of the temperature structure and chemical composition is of particular interest, for which a subsequent flight downwind of the initial pattern will be performed. A classical Lagrangian approach is not possible, since partly divergent flows can be expected in regions of exchange and mixing. However, the temporal development of static stability of the underlying synoptic structure associated with different stages of a breaking event will be investigated with focus on the relation of tropopause evolution and stability and their relation to transport and mixing.

To investigate the effects of the TIL on transport and mixing, the high-resolution (3D) temperature distribution from GLORIA and profiles from dropsondes are essential. These will be complemented by high resolution in-situ tracer profiles of particularly CO, O₃, CO₂, HCl and H₂O, curtain structure data of H₂O and O₃ from WALES, and 3D trace gas distributions from GLORIA such as H₂O and O₃.

We will use tomographic flight patterns which will provide 3-D maps of the thermal structure of the UTLS and the tropopause and TIL. These will be complemented by high resolution vertical profiles based on in-situ measurements. As a result three dimensional stability and temperature surfaces will be obtained, which can be compared to the tracer structure and heating rates deduced from the longwave irradiance from GLORIA. The comparison of regions with static stability maxima and characteristic gradient changes of tracer profiles will provide information on the effect of temperature structure on transport and mixing.

Central observations for this WP:

- Full payload

ST1_Q2:

Radiatively active tracers like ozone and water vapor can be exchanged across the extra-tropical tropopause by various processes with varying strengths during different seasons. This modifies the local temperature gradient on time scales of days thereby affecting the TIL structure. Therefore, observations from tomographic flights will be used to investigate potential formation mechanisms of the TIL. Flights under synoptically quiet conditions with a calm and well-defined tropopause will deliver the background state of temperature structure and tracer profiles. These data will be compared to data obtained at a later stage of a developing baroclinic wave containing different development stages and horizontal gradients of PV, stability and tracers. The combined data of temperature and tracer structure will elucidate the relation between stability and transport under different meteorological conditions.

Central observations for this WP:

- GLORIA (H₂O, O₃, cirrus, IR-radiance), WALES (H₂O, O₃, cirrus), min-DOAS (H₂O, cirrus), Dropsondes (Pressure/Temperature)

ST2_Q1:

The results of Ploeger et al. (2013) suggest a dominant transport pathway for moistening the extra-tropical UTLS during summer and fall related to the Asian monsoon and horizontal poleward transport. The study focused on the region above the subtropical jet however, the results imply a significant influence of horizontal transport from subtropical latitudes throughout the UTLS up to about 430 K during summer and fall in the northern hemisphere. This result is partly based on anti-correlations of simulated (CLaMS) zonal mean water vapor and ozone tendency time series. The anti-correlations are in reasonable agreement with corresponding values obtained from MLS satellite observations (Fig.9). However, the relatively broad weighting functions of MLS do not allow for observations of the fine structure provided by CLaMS simulations. This concerns, for example, the location of an area with a less pronounced anti-correlation around the extra-tropical TIL, which could be a hint to a shorter time scale of mixing. The WISE instrumentation and measurement concept is ideally suited to provide details of the underlying transport and mixing processes influencing the anti-correlation of water vapor and ozone tendencies in the area of the TIL and above. The quality of transport and mixing in CLaMS can be measured by testing the capability of the model to reproduce small-scale (3D) trace gas structures observed by GLORIA, 2D curtains from lidar observations, and tracer-tracer correlations from detailed in-situ observations. The CLaMS model alone provides useful information on both origin of air as well as the history of mixing (Vogel, et al., 2011, Konopka et al., 2012).

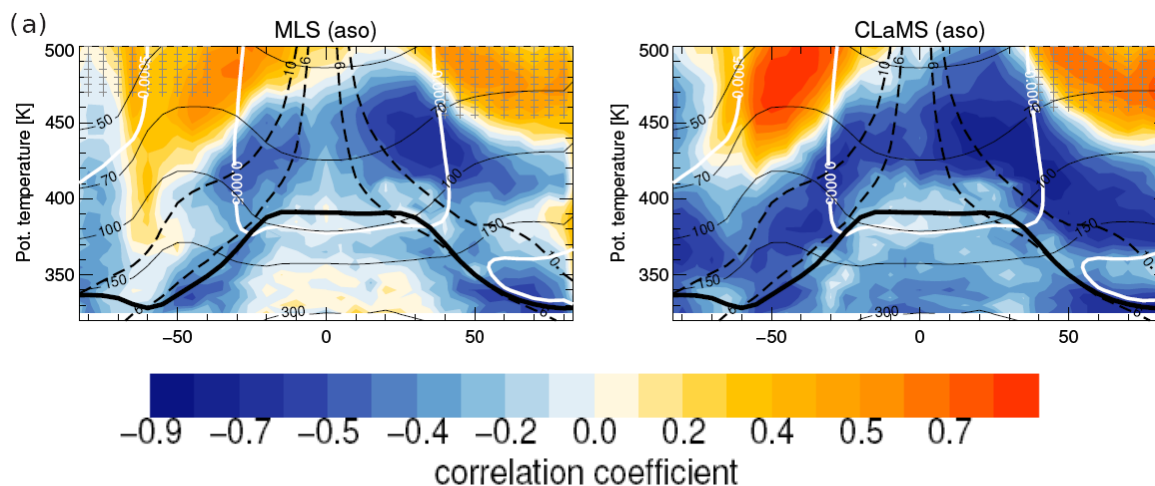


Figure 9: (a) Correlation coefficients (color coded) for the correlation between zonal mean MLS (left) and CLaMS (right) water vapor and ozone tendency time series at each latitude/ potential temperature location, for August–October ‘aso’ (2005–2010). Black lines show pressure, gray lines PV (± 6 , ± 10 PVU), white lines Brunt-Vaisala frequency N^2 ($5 \cdot 10^{-4} \text{ s}^{-2}$). Altitudes with mean water vapor at mid latitudes higher than at low latitudes are hatched with crosses. The zonal mean is based on the calculated tropopause (adapted from Ploeger et al., 2013).

Central observations for this WP:

- GLORIA (H_2O , O_3 , Tracer), WALES (H_2O , O_3), UMAQS (CO), AIMS (HCl), HAGAR-4 and GhOST-MS (tracer with a broad range of lifetimes)

ST2_Q2:

Further work shall quantify the impact of the Asian monsoon on the composition (e. g. water vapor) in the LMS. For this purpose, transport model tracers tagging the origin of air (Guenther et al., 2008) will be used to calculate which fraction of air in the extra-tropical LMS originated from the area of the Asian summer monsoon. Correlations of the monsoon tracer with observed and simulated water vapor will facilitate the interpretation of observations of enhanced water vapor values. The timing of the measurement campaign during September/October allows sampling the extra-tropical UTLS during the season of the largest impact of air masses from the Asian monsoon (e.g., Ploeger et al., 2013). Assessing the potential of the Asian monsoon circulation of transporting air into the lower stratosphere is also crucial to understand the pathways of anthropogenic pollutants into the lower stratosphere.

Furthermore, the comparison of three-dimensional observations of low latitude intrusions and filaments by GLORIA with the CLaMS model simulation will allow detailed process studies concerning the processes involved in the horizontal transport across the subtropical transport barrier. Such three-dimensional observations of filaments are novel, and the combination with the Lagrangian CLaMS model simulations provides an ideal basis for investigating the role of filamentary structures in trace gas exchange across the tropopause.

Central instruments for this WP:

- In-situ observations of monsoon tracers (e.g. UMAQS CH₄, HAGAR-4 CH₄ and NMHCs, Ghost-MS C₂Cl₄) and H₂O, long-lived stratospheric tracers like SF₆, CO₂, HCl to contrast aged air and recent mixing
- GLORIA 3-dimensional constituent fields

ST2_Q3:

In-situ measurements of a suite of tracers with a wide range of atmospheric lifetimes (several days to many years) will not only provide detailed information on the fine scale structure of the UTLS, but will allow to determine time scales and pathways of transport and mixing (including cross tropopause). The key technique to be employed in order to interpret the in situ measurements is the analysis of tracer-tracer correlations, which exhibit distinct branches in the troposphere and stratosphere. Furthermore, correlations between tracers with sufficiently different lifetimes are generally non-linear in the stratosphere and are shaped by the details and time scales of transport and mixing processes. In fact, Ehhalt et al, (2007) showed that using non-linear correlations between NMHC species with a suitable range of lifetimes it is possible to derive the spectrum of transport times (“age spectrum”). Furthermore individual mixing events can be detected and analysed as mixing lines in the correlation plots, provided sufficient precision and spatial resolution (<~1 min) of the measurements, which will be available for at least CO, H₂O, O₃, CO₂, CH₄, N₂O, SF₆, CFC-12, and several short-lived NMHCs. Concurrent simulations by the CLaMS model will aid the interpretation of the in situ measurements in terms of transport processes and meteorological context. At the same time, the in situ observations will serve to validate the model and optimize its mixing parametrization, thus increasing confidence in the simulation of transport and mixing.

- Essential: Tracer in situ measurements of tracers with different lifetimes: HAGAR-4, GhOST-MS, UMAQS, AIMS, FAIRO, FISH/HAI

ST3_Q1:

For WISE the University of Heidelberg group will particularly concentrate on the measurement of BrO (O₃, and NO₂), and total inorganic bromine will be estimated from simulations of the bromine partitioning with TOMCAT/SLIMCAT chemical transport model (CTM). BrO will be measured in limb scattered skylight, and the concentration of BrO (and of other gases) will be inferred using the novel developed O₃ scaling method, radiative transfer modelling (Deutschmann et al., 2011) and from optimal estimation (Werner et al., 2015). Total bromine will be assessed from inferred inorganic bromine and from organic bromine simultaneously by the University of Frankfurt. GhOST-MS measures all relevant bromine source gases (long and short lived) allowing to derive a complete organic bromine budget (e.g. Sala et al., 2014), as well as chlorine and iodine. The time resolution for the organic halogen species will be 4 minutes, with an integration time of about 1 minute. This will allow to derive the budget under different meteorological conditions and also as a function of altitude and distance to the tropopause. Total bromine will be assessed from inferred organic bromine and from inorganic bromine simultaneously derived from BrO measurements by the University of Heidelberg.

- Essential: mini DOAS, Ghost-MS, AIMS

ST4_Q1:

To investigate the link between wave breaking (and associated transport and water vapor) and cirrus formation at mid-latitudes, the unprecedented sensitivity of infrared limb sounders to detect extremely low IWC (*see above, Spang et al., 2012*) will be employed. The detection sensitivity might be even more sensitive than (space) lidars. Usually the vertical sampling and resolution is the main limiting factor for IR limb when exploring cirrus clouds and their exact location in respect to the tropopause, especially in comparison to the high resolved lidar measurements. However this handicap is eliminated with the imaging technique applied in the GLORIA instrument, where a vertical sampling of ~150 m at 10 km is achieved. In addition, the 3D/tomographic measurement and retrieval capability of GLORIA (Ungermann et al. 2011) can further improve the characterisation of the cloud structure. The downward looking measurements of the DIAL lidar will add substantial information on the macro and microphysical physical quantities (cloud top/base height, cloud phase, water vapour amount and estimates of ice water content. In combination with GLORIA observations, it will be possible to proof if LMS cirrus is existing and if the occurrence is currently substantially underestimated in satellite observations. The mini DOAS instrument will help to quantify the cirrus structure, which is essential for the radiation budget and also affects the heating rates (**Link to ST1**). Coincident measurements with the CALIPSO lidar can further quantify the potential deficit in global observations on LMS cirrus, which is also important for to know for validation studies of climate models like in the Cloud Feedback Model Intercomparison Program (CFMIP) (see <http://www.cfmip.net>, or e.g. Chepfer et al., 2012 (Q3.1; Q3.2))

- H₂O and cirrus by GLORIA, WALES and mini-DOAS, Temperature profiles by Drospondes and GLORIA

ST4_Q2:

HAI (**PTB Braunschweig**) will be used to investigate the conditions for the formation of cirrus particles. It will provide H₂O_{vap} with high spatial resolution in and around sub-visible cirrus clouds and in the tropopause region. HAI's data will be evaluated in cooperation with M. Riese/M. Krämer, FZJ, and thereby complement the FISH instrument, which measures total water (i.e gas and condensed phase) using a forward facing inlet. N₂O (**Mainz**) data will be used to distinguish between tropospheric and stratospheric air masses along the horizontal flight track. This is essential to identify e.g. the location of cirrus cloud occurrence and their relation to the tropopause from the in-situ data. The data will be further included in the cirrus modelling approach by FZ Jülich (R. Spang) and University Mainz to study the effects of water vapor on the occurrence of the TIL (D. Kunkel).

Central instruments for this WP are

- GLORIA and WALES, FISH, HAI, UMAQS

5 References

Aschmann, J., et al., Modeling the transport of very short-lived substances into the tropical upper troposphere and lower stratosphere, *Atmos. Chem. Phys.*, 9, 9237–9247, 2009.

Bell, S. W., and M. A. Geller, Tropopause inversion layer: Seasonal and latitudinal variations and representation in standard radiosonde data and global models, *J. Geophys. Res.*, 113, D05109, doi:10.1029/2007JD009022, 2008.

Anderson, J. G., D. M. Wilmouth, J. B. Smith, and D. S. Sayres (2012), UV dosage levels in summer: Increased risk of ozone loss from convectively injected water vapor, *Science*, 17, 835-839.

Birner, T., A. Dornbrack, and U. Schumann (2002), How sharp is the tropopause at midlatitudes?, *Geophys. Res. Lett.*, 29(14), 1700, doi:10.1029/2002GL015142.

Birner, T., D. Sankey, and T. G. Shepherd (2006), The tropopause inversion layer in models and analyses, *Geophys. Res. Lett.*, 33, L14804, doi:10.1029/2006GL026549.

Birner, T. (2010), Residual circulation and tropopause structure, *J. Atmos. Sci.*, 67, 2582–2600, doi:10.1175/2010JAS3287.1

Bönisch, H., A. Engel, J. Curtius, T. Birner, and P. Hoor (2009), Quantifying transport into the lowermost stratosphere using simultaneous in-situ measurements of SF₆ and CO₂, *Atmos. Chem. Phys.*, 9(16), 5905–5919, doi:10.5194/acp-9-5905-2009

Bönisch, H., et al., On the structural changes in the Brewer-Dobson circulation after 2000, *Atmos. Chem. Phys.*, 11, 3937-3948, doi:10.5194/acp-11-3937-2011, 2011.

Chagnon, J.M., Gray, S.L., and Methven, J.; Diabatic processes modifying potential vorticity in a North Atlantic cyclone; *Q.J.R. Met. Soc.*; doi:10.1002/qj.2037, 2012.

Chepfer, H., S. Bony, D. Winker, G. Cesana, J. L. Dufresne, P. Minnis, C. J. Stubenrauch, and S. Zeng: The GCM Oriented CALIPSO Cloud Product (CALIPSO-GOCCP), *J. Geophys. Res.*, 115, D00H16, doi:10.1029/2009JD012251, 2010.

Davis, S., Hlavka, D., Jensen, E., Rosenlof, K., Yang, Q., Schmidt, S., Borrmann, S., Frey, W., Lawson, P., Voemel, H., and Bui, T. P.: In situ and lidar observations of subvisible cirrus clouds during TC4, *J. Geophys. Res.*, 115, D00J17, doi:10.1029/2009JD013093, 2010.

Dessler, A. E., Clouds and water vapor in the Northern Hemisphere summertime stratosphere, *J. Geophys. Res.*, 114, D00H09, doi:10.1029/2009JD012075, 2009.

Dethof, A., A. O'Neill, J. M. Slingo, and H. G. J. Smit (1999), A mechanism for moistening the lower stratosphere involving the Asian summer monsoon, *Q. J. R. Meteorol. Soc.*, 125, 1079-1106.

Deutschmann, T., et al., (2011). The Monte Carlo Atmospheric Radiative Transfer Model McArtim: Introduction and Validation of Jacobians and 3D Features. *Journal of Quantitative Spectroscopy and Radiative Transfer*, Vol. 112, No. 6, 1119–1137.

Dorf, M., et al., (2008), Bromine in the tropical troposphere and stratosphere as derived from balloon-borne BrO observations, *Atmos. Chem. Phys.*, 8, 7265–7271.

Eckhardt S., A. Stohl, H. Wernli, P. James, C. Forster, N. Spichtinger, A 15-year climatology of warm conveyor belts. *J. Climate*, 17, 218-237, 2004.

Ehhalt, D. H., F. Rohrer, D. R. Blake, D. E. Kinnison, and P. Konopka (2007), On the use of nonmethane hydrocarbons for the determination of age spectra in the lower stratosphere, *J. Geophys. Res.*, 112, D12208, doi:10.1029/2006JD007686

Eichler, H., A. Ehrlich, M. Wendisch, G. Mioche, J.-F. Gayet, M. Wirth, C. Emde, and A. Minikin, 2009: Influence of ice crystal shape on retrieval of cirrus optical thickness and effective radius: A case study. *J. Geophys. Res.*, **114**, D19203, doi:10.1029/2009JD012215.

Eixmann, R., D. Peters, Ch. Zülicke, M. Gerding und A. Dörnbrack, On the upper tropospheric formation and occurrence of high and thin cirrus clouds during anticyclonic poleward Rossby wave breaking events, *Tellus*, 62 A, 228-242, doi:10.1111/j.1600-0870.2010.00437.x, 2010.

Engel, A., et al. (2006), Highly resolved observations of trace gases in the lowermost stratosphere and upper troposphere from the SPURT project: An overview, *Atmos. Chem. Phys.*, 6, 283–301, doi:10.5194/acp-6-2651-2006, 2006.

Erler, A., and V. Wirth (2011), The static stability of the tropopause region in adiabatic baroclinic life cycle experiments, *J. Atmos. Sci.*, 68(6), 1178–1193, doi:10.1175/2010JAS3694.1.

Fahey, D.W., et al., The AquaVIT-1 Intercomparison of Atmospheric Water Vapor Measurement Techniques, *Atmos. Meas. Tech.*, 7, 3177-3213, 2014.

Fischer, H., et al. (2000), Tracer correlations in the northern high latitude lowermost stratosphere: Influence of cross-tropopause mass exchange, *Geophys. Res. Lett.*, 27(1), 97–100.

Gabriel, A., and D. Peters: A diagnostic study of different types of Rossby wave breaking events in the northern extra-tropics, *J. Meteor. Soc. Japan*, 86, 613–631, 2008.

Gettelman, A., P. Hoor, L. L. Pan, W. J. Randel, M. I. Hegglin, and T. Birner (2011), The extratropical upper troposphere and lower stratosphere, *Rev. Geophys.*, 49, RG3003.

Grise, K.M., D.W.J. Thompson, T. Birner, A Global Survey of Static Stability in the Stratosphere and Upper Troposphere, *J. Climate*, 23, 2275-2292, 2010.

Günther, G., R. Müller, M. von Hobe, F. Stroh, P. Konopka, and C. M. Volk (2008), Quantification of transport across the boundary of the lower stratospheric vortex during Arctic winter 2002/2003, *Atmos. Chem. Phys.*, 8 (13), 3655-3670.

Haynes, P., and E. Shuckburgh (2000), Effective diffusivity as a diagnostic of atmospheric transport 2. Troposphere and lower stratosphere, *J. Geophys. Res.*, 105 (D18), 22,795-22,810.

- Hegglin, M. I., et al. (2004), Tracing troposphere to stratosphere transport within a mid-latitude deep convective system, *Atmos. Chem. Phys.*, 4, 741–756.
- Hegglin, M. I., C. D. Boone, G. L. Manney, and K. A. Walker (2009), A global view of the extratropical tropopause transition layer from Atmospheric Chemistry Experiment Fourier Transform Spectrometer O₃, H₂O, and CO, *J. Geophys. Res.*, 114, D00B11, doi:10.1029/2008JD009984.
- Hegglin, M.I., and T.G. Shepherd, Large climate-induced changes in UV index and stratosphere-to-troposphere ozone flux, *Nature Geoscience*, 2, 687-691, 2009.
- Homan, C. D., et al., Tracer measurements in the tropical tropopause layer during the AMMA/SCOUT-O₃ aircraft campaign, *Atmos. Chem. Phys.*, 10, 3615–3627, doi:10.5194/acp-10-3615-2010, 2010.
- Homeyer, C. R., and K. P. Bowman (2012), Rossby wave breaking and transport between the tropics and extratropics above the subtropical jet, *J. Atmos. Sci.*, 70, 607-626.
- Hoor, P., Fischer, H., Lange, L., Lelieveld, J., Brunner, D., Seasonal variations of a mixing layer in the lowermost stratosphere as identified by the CO-O₃ correlation from in situ measurements, *J. Geophys. Res.*, 107 (D5-D6), 4044, 2002
- Hoor, P., C. Gurk, D. Brunner, M. I. Hegglin, H. Wernli, and H. Fischer (2004), Seasonality and extent of extratropical TST derived from in situ CO measurements during SPURT, *Atmos. Chem. Phys.*, 4(5), 1427–1442, doi:10.5194/acp-4-1427-2004.
- Hoor, P., H. Fischer, and J. Lelieveld (2005), Tropical and extratropical tropospheric air in the lowermost stratosphere over Europe: A CO-based budget, *Geophys. Res. Lett.*, 32, L07802, doi:10.1029/2004GL022018.
- Hoor, P., H. Wernli, M. I. Hegglin, and H. Bönisch (2010), Transport timescales and tracer properties in the extratropical UTLS, *Atmos. Chem. Phys.*, 10(16), 7929–7944.
- Hossaini, R., et al., Efficiency of short-lived halogens at influencing climate through depletion of stratospheric ozone. *Nature Geoscience*, Vol. 8, No. 2, 186 – 190, 2015.
- Joos, H, and H. Wernli; Influence of microphysical processes on the potential vorticity development in a warm conveyor belt: a case-study with the limited area model COSMO, *Q.J.R. Meteorolo. Soc.*, 138: 4017-418, doi:10.1002/qj.934, 2012.
- Keckhut, P., Hauchecorne, A., Bekki, S., Colette, A., David, C., and Jumelet, J.: Indications of thin cirrus clouds in the stratosphere at mid-latitudes, *Atmos. Chem. Phys.*, 5, 3407-3414, doi:10.5194/acp-5-3407-2005, 2005.
- Konopka, P., et al., (2009), Annual cycle of horizontal in-mixing into the lower tropical stratosphere, *J. Geophys. Res.*, 114, D19111, doi: 10.1029/2009JD011955.
- Konopka, P., et al., (2010), Annual cycle of ozone at and above the tropical tropopause: observations versus simulations with the Chemical Lagrangian Model of the Stratosphere (CLaMS), *Atmos. Chem. Phys.*, 10(1), 121–132, doi:10.5194/acp-10-121-2010.
- Konopka, P., and L. L. Pan (2012), On the mixing-driven formation of the Extratropical Transition Layer (ExTL), *J. Geophys. Res.*, 117, doi:10.1029/2012JD017876.

Kunkel, D., P. Hoor, and V. Wirth (2014), Can inertia-gravity waves persistently alter the tropopause inversion layer?, *Geophys. Res. Lett.*, 41, 7822–7829, doi:10.1002/2014GL061970.

Kunkel, D., Hoor, P., and Wirth, V.: The tropopause inversion layer in baroclinic life-cycle experiments: the role of diabatic processes, *Atmos. Chem. Phys.*, 16, 541-560, doi:10.5194/acp-16-541-2016, 2016.

Kunz, A., P. Konopka, R. Müller, L. L. Pan, C. Schiller, and F. Rohrer (2009), High static stability in the mixing layer above the extratropical tropopause, *J. Geophys. Res.*, 114, D16305, doi:10.1029/2009JD011840

Laube, J. C., et al., (2008) Contribution of very short-lived organic substances to stratospheric chlorine and bromine in the tropics - a case study, *Atmos. Chem. Phys.*, 8, 7325–7334, 2008.

Levine, J. G., et al., Pathways and timescales for troposphere-to-stratosphere transport via the tropical tropopause layer and their relevance for very short lived substances, *J. Geophys. Res.*, 112, doi: 10.1029/2005JD006940, 2007.

Liang, Q., et al., Convective transport of very short lived bromocarbons to the stratosphere, *Atmos. Chem. Phys.*, 14, 5781–5792, doi:10.5194/acp-14-5781-2014, <http://www.atmos-chem-phys.net/14/5781/2014/>, 2014

McIntyre, M. E., and T. N. Palmer (1983), Breaking planetary waves in the stratosphere, *Nature*, 305, 593-600.

McKenna, D. S., P. Konopka, J.-U. Grooss, G. Günther, R. Müller, R. Spang, D. Offermann, and Y. Orsolini (2002b), A new Chemical Lagrangian Model of the Stratosphere (CLaMS): 1. Formulation of advection and mixing, *J. Geophys. Res.*, 107 (D16), 4309.

Miyazaki, K., S. Watanabe, Y. Kawatani, Y. Tomikawa, M. Takahashi, and K. Sato (2010), Transport and mixing in the extratropical tropopause region in a high-vertical-resolution GCM. Part I: Potential vorticity and heat budget analysis, *J. Atmos. Sci.*, 67(5), 1293–1314.

Montoux, N., P. Keckhut, A. Hauchecorne, J. Jumelet, H. Brogniez, and C. David: Isentropic modeling of a cirrus cloud event observed in the midlatitude upper troposphere and lower stratosphere, *J. Geophys. Res.*, 115, D02202, doi:10.1029/2009JD011981, 2010.

Noel, V., and M. Haefelin: Midlatitude cirrus clouds and multiple tropopauses from a 2002 – 2006 climatology over the SIRTa observatory, *J. Geophys. Res.*, 112, D13206, doi:10.1029/2006JD007753, 2007.

Müller, S., et al., In situ detection of stratosphere-troposphere exchange of cirrus particles in the midlatitudes, *Geophys. Lett.*, 42, doi:10.1002/2014GL062556, 2015

Müller, S., Hoor, P., Bozem, H., Gute, E., Vogel, B., Zahn, A., Bönisch, H., Keber, T., Krämer, M., Rolf, C., Riese, M., Schlager, H., and Engel, A.: Impact of the Asian monsoon on the extratropical lower stratosphere: trace gas observations during TACTS over Europe 2012, *Atmos. Chem. Phys.*, 16, 10573-10589, doi:10.5194/acp-16-10573-2016, 2016.

Pan, L. L., S. Solomon, W. Randel, J.-F. Lamarque, P. Hess, J. Gille, E.-W. Chiou, and M. P. McCormick (1997), Hemispheric asymmetries and seasonal variations of the lowermost stratospheric water vapor and ozone derived from SAGE II data, *J. Geophys. Res.*, 102 (D23)

Pan, L. L., W. J. Randel, B. L. Gary, M. J. Mahoney, and E. J. Hintsa (2004), Definitions and sharpness of the extratropical tropopause: A trace gas perspective, *J. Geophys. Res.*, 109, D23103, doi:10.1029/2004JD004982.

Pan, L. L., et al. (2007), Chemical behavior of the tropopause observed during the Stratosphere-Troposphere Analyses of Regional Transport experiment, *J. Geophys. Res.*, 112, D18110, doi:10.1029/2007JD008645

Pan, L. L., W. J. Randel, J. C. Gille, B. N. W. D. Hall, S. Massie, V. Yudin, R. Khosravi, P. Konopka, and D. Tarasick (2000 Pisso, I., et al., Emission location dependent ozone depletion potentials for very short-lived halogenated species, *Atmos. Chem. Phys.*, 10, 12 025–12 036, doi: 10.5194/acp-10-12025-2010, <http://www.atmos-chem-phys.net/10/12025/2010/>, 2010.

Platt, U. and J. Stutz (2008). *Differential Optical Absorption Spectroscopy (DOAS), Principle and Applications*. Number ISBN 3- 340-21193-4. Heidelberg: Springer Verlag.9), Tropospheric intrusions associated with the secondary tropopause, *J. Geophys. Res.*, 114, D10302.

Pan, L. L., and L. A. Munchak: Relationship of cloud top to the tropopause and jet structure from CALIPSO data, *J. Geophys. Res.*, 116, D12201, doi:10.1029/2010JD015462, 2011.

Ploeger, F., et al. (2011), Insight from ozone and water vapour on transport in the tropical tropopause layer (TTL), *Atmos. Chem. Phys.*, 11, 407-419, doi:10.5194

Ploeger, F., et al. (2013), Horizontal water vapor transport in the lower stratosphere from subtropics to high latitudes during boreal summer, *J. Geophys. Res.*, accepted.

Postel, G. A., and M. H. Hitchman (1999), A climatology of Rossby wave breaking along the subtropical tropopause, *J. Atmos. Sci.*, 56, 359-373.

Randel, W. J., F. Wu, A. Gettelman, J. Russell, J. Zawodny, and S. Oltmans (2001), Seasonal variation of water vapor in the lower stratosphere observed in Halogen Occultation Experiment data, *J. Geophys. Res.*, 106, D13.

Randel, W. J., F. Wu, and P. Forster (2007), The extratropical tropopause inversion layer: Global observations with GPS data, and a radiative forcing mechanism, *J. Atmos. Sci.*, 64, doi:10.1175/2007JAS2412.1

Randel, W. J., and F. Wu (2010), The polar summer tropopause inversion layer, *J. Atmos. Sci.*, 67, 2572- 2581.

Ray, E. A., F. L. Moore, J. W. Elkins, G. S. Dutton, D. W. Fahey, H. Vömel, S. Oltmans, and K. H. Rosenlof (1999), Transport into the northern hemisphere lowermost stratosphere revealed by in situ tracer measurements, *J. Geophys. Res.*, 104, 26,565-26,580.

Riese, M., F. Ploeger, A. Rap, B. Vogel, P. Konopka, M. Dameris, and P. Forster (2012), Impact of uncertainties in atmospheric mixing on simulated UTLS composition and related radiative effects, *J. Geophys. Res.*, 117, D16305, doi:10.1029/2012JD017751

Riese, M., G. L. Manney, J. Oberheide, X. Tie, R. Spang, and V. Küll (2002), Stratospheric transport by planetary wave mixing as observed during CRISTA-2, *J. Geophys. Res.*, 107, 8179.

Riese, M., et al., Gimballed Limb Observer for Radiance Imaging of the Atmosphere (GLORIA) scientific objectives, *Atmos. Meas. Tech.*, 7, 1915-1928, doi:10.5194/amt-7-1915-2014, 2014.

Rolf, C., et al., Transport of Antarctic stratospheric strongly dehydrated air into the troposphere observed during the HALO-ESMVal campaign 2012, *Atmos. Chem. Phys.*, Vol. 15, doi:10.5194/acp-15-9143-2015, 9143-9158, 2015.

Rosenlof, K. H., A. F. Tuck, K. K. Kelly, J. M. Russell III, and M. P. McCormick (1997), Hemispheric asymmetries in the water vapor and inferences about transport in the lower stratosphere, *J. Geophys. Res.*, 102, 13,213-13,234.

Schwartz, M. J., W. G. Read, M. L. Santee, N. J. Livesey, L. Froidevaux, A. Lambert and G. L. Manney (2013), Convectively injected water vapor in the North American summer lowermost stratosphere, *Geophys. Res. Lett.*, 40, 1-6.

Solomon, S., K. H. Rosenlof, R. W. Portmann, J. Daniel, S. M. Davis, T. J. Sanford, and G. K. Plattner (2010), Contributions of stratospheric water vapor to decadal changes in the rate of global warming, *Science*, 327, 1219-1223.

Son, S. W., and L. M. Polvani (2007), Dynamical formation of an extra-tropical tropopause inversion layer in a relatively simple general circulation model, *Geophys. Res. Lett.*, 34, L17806, doi:10.1029/2007GL030564.

Spang, R., Riese, M., Eidmann, G., Offermann, D., Pfister, L., and Wang, P. H.: CRISTA observations of cirrus clouds around the tropopause, *J. Geophys. Res.*, 107, 8174, doi:10.1029/2002JD000698, 2002.

Spang, R., L. Hoffmann, A. Kullmann, F. Olschewski, P. Preusse, P. Knieling, S. Schroeder, F. Stroh, K. Weigel, M. Riese: High resolution limb observations of clouds by the CRISTA-NF experiment during the SCOUT-O3 Tropical Aircraft campaign, *Adv. Space Res.*, 42 (2008), pp. 1765–1775, 2007.

Spang, R., et al., Satellite observations of cirrus clouds in the Northern Hemisphere lowermost stratosphere, *Atmos. Chem. Phys.*, 15, 927-950, doi:10.5194/acp-15-927-2015, 2015.

Spichtinger, P., K. Gierens, H. Wernli: A case study on the formation and evolution of ice supersaturation in the vicinity of a warm conveyor belt's outflow region. *Atmos. Chem. Phys.*, 5, 973-987, 2005.

Sprung, D., and A. Zahn (2010), Acetone in the upper troposphere/ lowermost stratosphere measured by the CARIBIC passenger aircraft: Distribution, seasonal cycle, and variability, *J. Geophys. Res.*, 115, D16301, doi:10.1029/2009JD012099

Strahan, S. E., Duncan, B. N., Hoor; P., Observationally derived transport diagnostics for the lowermost stratosphere and their application to the GMI chemistry and transport model, *Atmos Chem Phys.*, 7, 2435-2445, 2007.

Thouret, V., J.-P. Camma, B. Sauvage, G. Athier, R. Zbinden, P. Nalec, P. Simon, and F. Karcher, Tropopause referenced ozone climatology and inter-annual variability (1994-2003) from the MOZAIC programme, *Atmos. Chem. Phys.*, 1412 5, 5441–5488, 2005

Ungermann, J., Blank, J., Lotz, J., Leppkes, K., Hoffmann, L., Guggenmoser, T., Kaufmann, M., Preusse, P., Naumann, U., and Riese, M.: A 3-D tomographic retrieval approach with advection compensation

for the air-borne limb-imager GLORIA, *Atmos. Meas. Tech.*, 4, 2509-2529, doi:10.5194/amt-4-2509-2011, 2011.

Ungermann, J., et al., Filamentary structure in chemical tracer distributions near the subtropical jet following a wave breaking event, *Atmos. Chem. Phys.*, 13, 10517-10534, doi:10.5194/acp-13-10517-2013, 2013.

Vogel, B., et al. (2011), Transport pathways and signatures of mixing in the extratropical tropopause region derived from Lagrangian model simulations, *J. Geophys. Res.*, 116, doi:10.1029/2010JD014876

Vogel, B., Günther, G., Müller, R., Grooß, J.-U., Hoor, P., Krämer, M., Müller, S., Zahn, A., and Riese, M.: Fast transport from Southeast Asia boundary layer sources to northern Europe: rapid uplift in typhoons and eastward eddy shedding of the Asian monsoon anticyclone, *Atmos. Chem. Phys.*, 14, 12745-12762, doi:10.5194/acp-14-12745-2014, 2014.

Vogel, B., Günther, G., Müller, R., Grooß, J.-U., Afchine, A., Bozem, H., Hoor, P., Krämer, M., Müller, S., Riese, M., Rolf, C., Spelten, N., Stiller, G. P., Ungermann, J., and Zahn, A.: Long-range transport pathways of tropospheric source gases originating in Asia into the northern lower stratosphere during the Asian monsoon season 2012, *Atmos. Chem. Phys.*, 16, 15301-15325, doi:10.5194/acp-16-15301-2016, 2016.

Volk, C. M., et al., Quantifying transport between the tropical and mid latitude lower stratosphere, *Science*, 272, 1763–1768, 1996.

Wang, T., and A. E. Dessler: Analysis of cirrus in the tropical tropopause layer from CALIPSO and MLS data: A water perspective, *J. Geophys. Res.*, 117, D04211, doi:10.1029/2011JD016442, 2012.

Waugh, D. W. (1996), Seasonal variation of isentropic transport out of the tropical stratosphere, *J. Geophys. Res.*, 101, 4007-4023

Wendisch, M., P. Yang, and P. Pilewskie: Effects of ice crystal habit on thermal infrared radiative properties and forcing of cirrus. *J. Geophys. Res.*, 112, D08201, doi:10.1029/2006JD007899, 2008.

Wendisch, M., D. Müller, D. Schell, and J. Heintzenberg, 2001: An airborne spectral albedometer with active horizontal stabilization. *J. Atmos. Ocean. Tech.*, **18**, 1856-1866.

Werner A., et al., Quantifying transport into the Arctic lowermost stratosphere, *Atmos. Chem. Phys.*, 10, 11623-11639, doi:10.5194/acp-10-11623-2010, 2010.

Weidner, F., et al., Balloon-borne Limb profiling of UV/vis skylight radiances, O₃, NO₂, and BrO: Technical set-up and validation of the method, *Atmos. Chem. Phys.*, 5, 1409–1422, 2005.

Werner, B., et al., Probing the subtropical lowermost stratosphere, tropical upper troposphere, and tropopause layer for inorganic bromine, *ACPD* (submitted), 2015. Wirth, V. (2003), Static stability in the extratropical tropopause region, *J. Atmos. Sci.*, 60, 1395–1409

Wirth, V., Szabo, T., Sharpness of the extratropical tropopause in baroclinic life cycle experiments, *Geophys. Res. Lett.*, 34, 2, L02809, DOI: 10.1029/2006GL028369, 2007.

Zahn, A., and C. A. M. Brenninkmeijer (2003), New directions: A chemical tropopause defined, *Atmos. Env.*, 37, 439–440

Appendix A: Specification of Instruments

The remote-sensing package consists of instruments covering a wide spectral range from the infrared to UV, thereby providing a large number of chemical species, including water vapor, ozone, transport tracers, cloud parameters as well as upwelling and downwelling spectral radiance. It is complemented by a suite of in-situ-observations focusing on water vapour and cloud particles as well as transport tracers. The following remote sensing and insitu instruments are part of the WISE payload.

Remote sensing:

- **GLORIA-AB** as an imaging FTIR spectrometer can provide high resolution (typically 300 m vertical resolution; 30 km x 30 km horizontally in tomographic mode) information on the chemical composition below the aircraft, allowing much better coverage than previously available. The list of species measurable by this IR limb imaging technique includes: Temperature, H₂O, HDO, CIRRUS (Ext., IWC), Ozone, PAN, CH₄, N₂O, CFC-11, CFC-12, HCFC-12, SF₆, C₂H₆, CH₃OH, CH₂O, NH₃, NO₂ (strat), N₂O₅ (strat), ClONO₂ (strat), BrONO₂ (strat), and HO₂NO₂ (strat). The uncertainty of temperature data is in the order of 0.5 K.
- **WALES** is a state-of-the-art differential absorption lidar (DIAL) that combines the measurement of water vapor and ozone profiles as well as aerosol optical properties with high vertical (~100m) and horizontal resolution (~10km) from the ground to the lower stratosphere.
- The **Mini-DOAS** instrument is an optical 6 channel spectrometer that analyzes in NADIR and Limb direction skylight of the UV/Vis/near-IR spectral range. Target species parameters are tropospheric column amounts (NADIR) and profiles (LIMB) of the species listed in the appendix A.

In-situ:

- The Fast In-situ Stratospheric Hygrometer (**FISH**) of Forschungszentrum Jülich is based on the Lyman-alpha photofragment fluorescence technique. The instrument is used for almost two decades from balloons and various aircraft -including the Geophysica, the DLR Falcon, the German Learjet and HALO as well as the NASA WB-57- for high-precision measurements of water vapour in the UTLS. The instrument was compared to several other in-situ and remote sensing instruments in atmospheric and laboratory experiments.
- The Hygrometer for Atmospheric Investigations (**HAI**) is a new development for HALO in cooperation of the Physikalisch-Technische Bundesanstalt Braunschweig (PTB) and

the Forschungszentrum Jülich, supported by the HALO-SPP. It is based on the tuneable diode laser absorption spectroscopy and primarily designed for measurements of gas-phase water in an open-path cell and thus a complement to the closed path gas phase/total water measurements of FISH in the cirrus altitude range. The instrument is equipped with two lasers at 1.4 μm and 2.6 μm wavelength in order to provide a large sensitivity range for water measurements reaching from the ground up to the UTLS. In addition, HAI contains a closed path cell using the same two lasers to additionally measure gas phase/total water in mixed phase and warm cloud levels.

- The Fast and Accurate In-situ Ozone instrument (**FAIRO**, KIT) contains a fast and precise (precision: typically <1% at 10 Hz) chemiluminescence detector and an accurate dual-beam UV photometer.
- The **AIMS** (Atmospheric chemical Ionization Mass Spectrometer) will provide fast measurements of the atmospheric HCl mixing ratio and other trace species such as HNO_3 , SO_2 , ClONO_2 . It is calibrated for HCl, HNO_3 and SO_2 in flight (and on ground) and has a time resolution of 1 Hz. The instrument has recently been developed and was successfully deployed in various missions on the Falcon and the HALO aircraft. Alternatively to HCl, the mass spectrometer can be driven in the water vapor mode. Water vapor down to <0.5 ppmv is detected with a high accuracy using an in-flight H_2O calibration system and a backward facing inlet. In addition, total water is measured with a forward facing inlet with the tunable diode laser TDL instrument WARAN (WVSS2 from Spectra Systems), which is integrated in the AIMS rack.
- The AENEAS instrument (AtmosphERIC Nitrogen oxides mEAsuring System) is a two channel chemiluminescence detector for the detection of NO. One channel is equipped with a gold converter for the conversion of reactive nitrogen species (NOy).
- The in-situ GC/MS **GHOST-MS** measures a wide suite of chemical tracers with different lifetimes from several days (CH_3I) to weeks, months and years, which can provide information on transport on different timescales. For the halocarbons (e.g. CH_3Br , CH_2Br , CFCs etc.) the temporal resolution is currently 4 minutes, while SF_6 and CFC-12 are measured with a temporal resolution of 1 minute. The instrument was operated successfully during all TACTS/ESMVal flights.
- **UMAQS** is a two channel quantum cascade laser IR absorption spectrometer capable of simultaneous high precision measurements of CO and N_2O , at 3 Hz and will be extended by an NDIR CO_2 instrument. The instrument was successfully operated on the FALCON aircraft during PGS 2015/2016 and DEEPWAVE and onboard the Lear Jet during AIRTOSS.
- **HAGAR-4** measures a large array of tracers with chemical time scales ranging from days to practically infinity. The instrument comprises of three modules employing different measurement techniques: i) two GC-ECD channels measuring SF_6 , CH_4 , H_2 ,

N₂O, CFC-11, CFC-12 and Halon-1211 every 90 s (precision ~1%), ii) a dual channel GC/MS measuring several short-lived non-methane hydrocarbons (NMHCs) every ~60 s, and iii) a non-dispersive IR detector measuring CO₂ at high time resolution (every 3 s) and with high accuracy (~0.1 ppm). HAGAR-4 is an extension of the HAGAR instrument (which lacks the GC/MS module) that has been operated extensively on the M55 Geophysica since 1998.

- **KITsonde:** KITsonde is a new modular multi-sensor Dropsonde system developed for HALO. KITsonde allows high-resolution measurements of temperature, humidity, wind and pressure with up to 4 sondes launched at one release and up to 30 active sondes at the same time. Measurement frequency is 1Hz which equals to a vertical resolution of ~5 m. Resolution (accuracy) is 0.1 K (< 0.2 K) for temperature, 1 %rH (<5 %rH) for humidity. Accuracy for pressure is <0.3 hPa, for wind speed < 0.2 ms⁻¹, and < 5 m (< 10 m) for horizontal position (geopotential height). The instrument was successfully operated aboard Dornier 128-6 research aircraft of Technical University of Braunschweig.

Table 1: WISE payload

Parameter	Instrument	Partner	Pis
Remote sensing			
H ₂ O, Cirrus, CFCs, O ₃ , PAN, HNO ₃ , N ₂ O, CH ₄ , Temperature,...	GLORIA-AB	JÜLICH / KIT	Preusse, Oelhaf
H ₂ O, Ozone, Cirrus	WALES Lidar	DLR	Fix, Wirth
H ₂ O (g,l,s), O ₃ , NO ₂ , HONO, CH ₂ O, IO, OIO, OclO, BrO, O ₄	Mini-DOAS	Uni Heidelberg	Pfeilsticker
In-situ			
H₂O and related			
H ₂ O (total + gas phase)	FISH	JÜLICH	Krämer
H ₂ O (gas phase)	HAI	PTB Braunschweig	Ebert
Pressure, temperature, humidity, wind (profiles)	Drop sonde	DLR	Busen
Tracer and others			
Ozone	FAIRO	KIT	Zahn
NO, NO _y	AENEAS	DLR	Ziereis
SF ₆ , F12, CH ₂ Br ₂ , CHBr ₃ , C ₂ Cl ₄ , ...	GhOST-MS	Uni Frankfurt	Engel
CO, CH ₄ , N ₂ O, CO ₂	UMAQS	Uni Mainz / MPI Mainz	Hoor / Fischer
HCl, HNO ₃ , SO ₂ or alternatively H ₂ O (gas phase and total)	AIMS	DLR / Uni Mainz	Voigt
CO ₂ , SF ₆ , CH ₄ , H ₂ , N ₂ O, CFC-11, CFC-12, Halon-1211 and several NMHCs	HAGAR-4	Uni Wuppertal	Volk